Supporting Information

Syntheses of three new isostructural lanthanide coordination polymers with tunable emission colours through bimetallic doping, and luminescent sensing properties

Ge Liu, Yu-Ke Lu, Yao-Yu Ma, Xiao-Qing Wang, Lei Hou* and Yao-Yu Wang

Key Laboratory of Synthetic and Natural Functional Molecule Chemistry of the Ministry of Education, Shaanxi Key Laboratory of Physico-Inorganic Chemistry, College of Chemistry & Materials Science, Northwest University, Xi'an 710069, P. R. China. Email: lhou2009@nwu.edu.cn

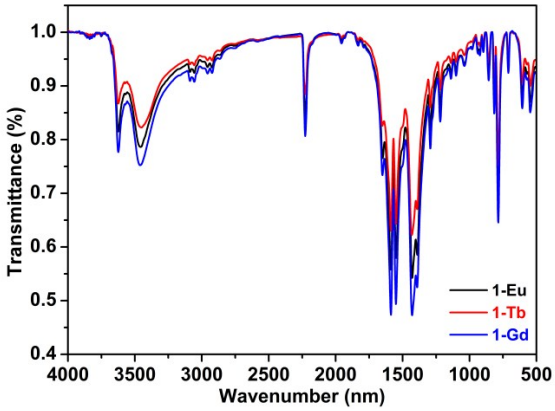

Figure S1. IR spectra of **1-Ln**.

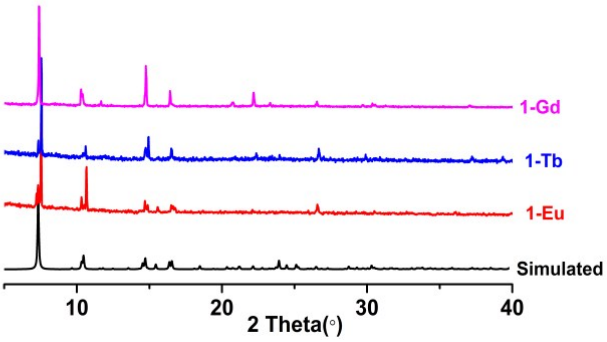

Figure S2. PXRD patterns of **1-Ln**.

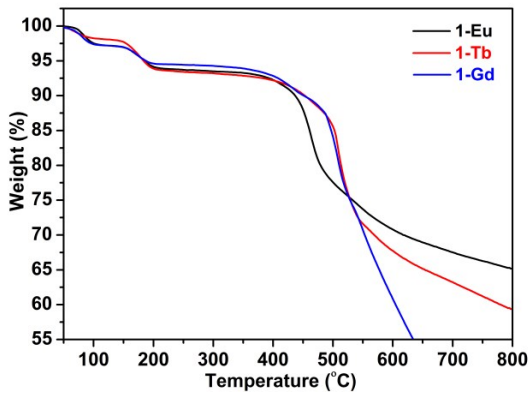

Figure S3. TGA curve of **1-Ln**.

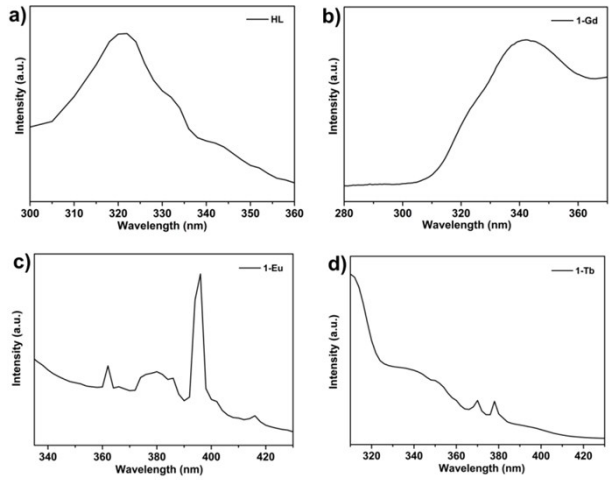

Figure S4. Excitation spectra of HL (a), **1-Eu** (b), **1-Gd** (c) and **1-Tb** (d).

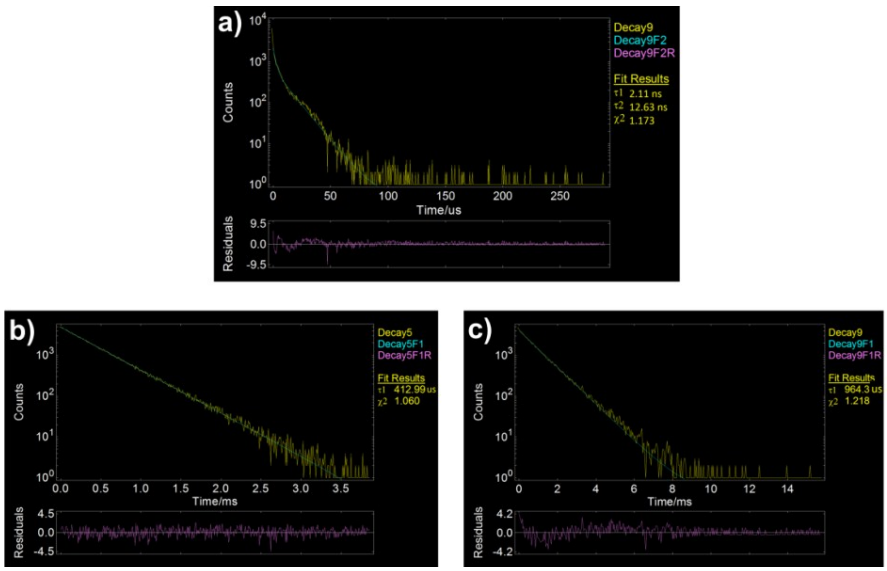

Figure S5. Luminescence decay lifetimes of **1-Gd** (a), **1-Eu** (b) and **1-Tb** (c).

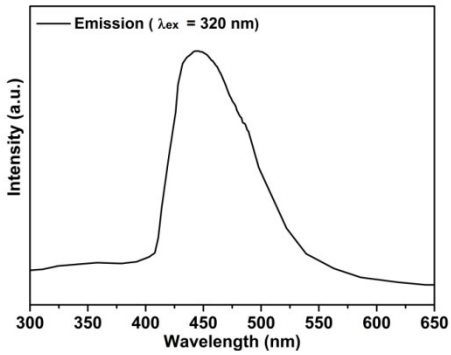

Figure S6. Solid state phosphorescent emission spectra of **1-Gd** at 77 K.

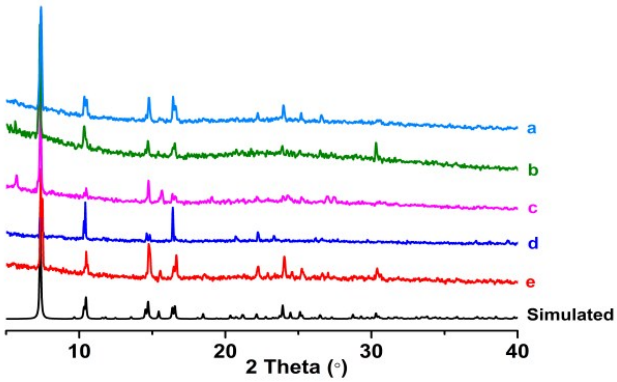

Figure S7. PXRD patterns of doped **1-Tb$_x$Eu$_{1-x}$** samples.

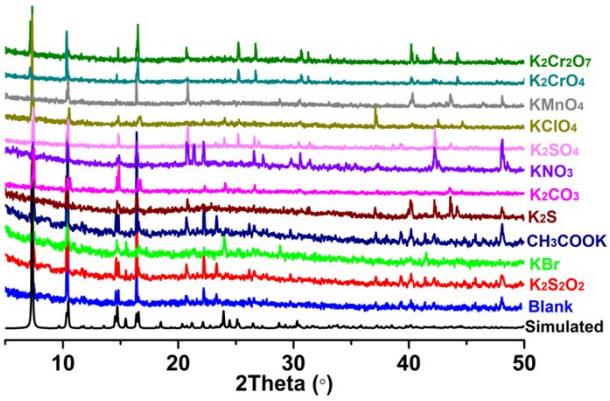

Figure S8. PXRD of **1-Eu** treated by different aqueous solutions.

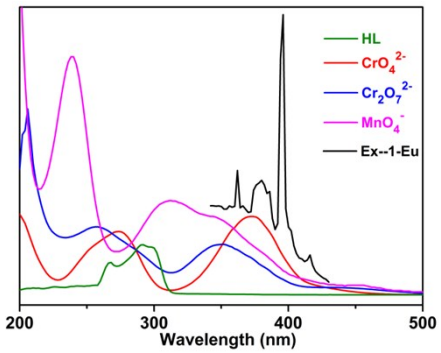

Figure S9. UV-vis adsorption spectra of HL, MnO_4^-, CrO_4^{2-} and $Cr_2O_7^{2-}$ in water, and the excitation spectrum of **1-Eu** in water.

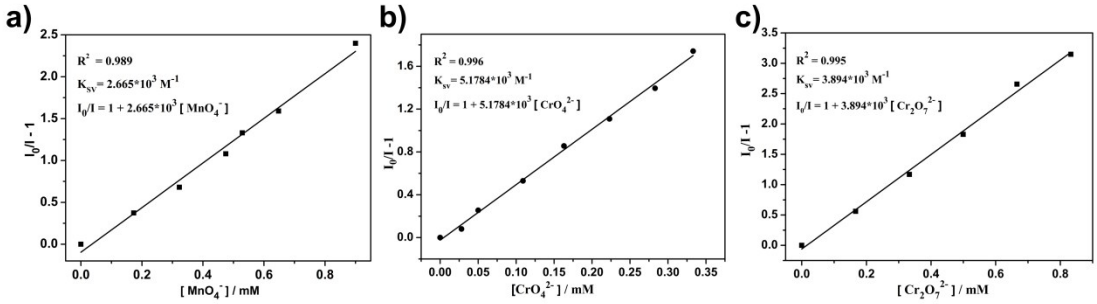

Figure S10. The linear correlation for the plot of (I_0/I)-1 vs concentration of MnO_4^- (a), CrO_4^{2-} (b) and $Cr_2O_7^{2-}$ (c), respectively, in low concentration range.

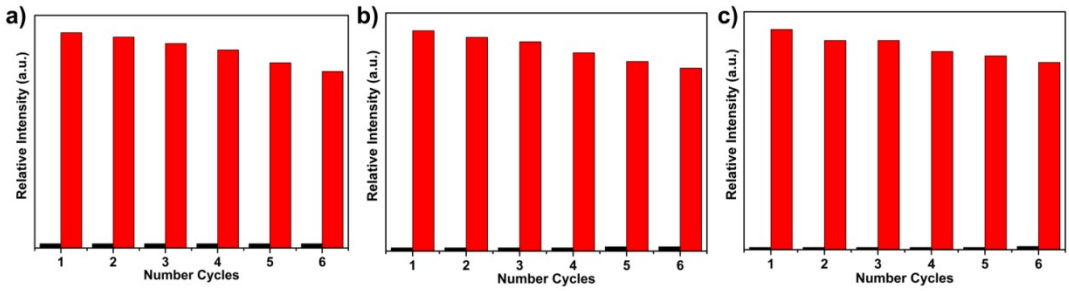

Figure S11. Multiple cycles for the fluorescence quenching of **1-Eu** by MnO_4^- (a), CrO_4^{2-} (b) and $Cr_2O_7^{2-}$ (c), and recovery after washing by water for six times.

Table S1. Selected bond lengths [Å] and angles [°] for **1-Ln**.

		1-Eu			
Eu(1)-O(5)	2.3515(12)	Eu(1)-O(4)#2	2.4175(13)	Eu(1)-O(1)	2.5929(12)
Eu(1)-O(6)#1	2.3817(12)	Eu(1)-O(1W)	2.4772(14)	Eu(1)-O(3)	2.4000(13)
Eu(1)-O(1)#2	2.3987(13)	Eu(1)-O(2)	2.4933(13)	Eu(1)-O(2W)	2.5472(13)
O(5)-Eu(1)-O(6)#1	86.31(4)	O(1)#2-Eu(1)-O(1W)	140.92(5)	O(4)#2-Eu(1)-O(2W)	129.03(5)
O(5)-Eu(1)-O(1)#2	91.69(4)	O(3)-Eu(1)-O(1W)	137.94(5)	O(1W)-Eu(1)-O(2W)	127.84(5)
O(6)#1-Eu(1)-O(1)#2	147.28(5)	O(4)#2-Eu(1)-O(1W)	68.56(5)	O(2)-Eu(1)-O(2W)	128.76(4)
O(5)-Eu(1)-O(3)	136.91(5)	O(5)-Eu(1)-O(2)	143.28(5)	O(5)-Eu(1)-O(1)	141.59(4)
O(6)#1-Eu(1)-O(3)	83.85(4)	O(6)#1-Eu(1)-O(2)	73.83(4)	O(6)#1-Eu(1)-O(1)	124.62(4)
O(1)#2-Eu(1)-O(3)	75.46(4)	O(1)#2-Eu(1)-O(2)	121.56(4)	O(1)#2-Eu(1)-O(1)	74.04(5)
O(5)-Eu(1)-O(4)#2	71.53(4)	O(3)-Eu(1)-O(2)	72.24(5)	O(3)-Eu(1)-O(1)	74.65(4)
O(6)#1-Eu(1)-O(4)#2	136.44(5)	O(4)#2-Eu(1)-O(2)	102.08(5)	O(4)#2-Eu(1)-O(1)	70.17(4)
O(1)#2-Eu(1)-O(4)#2	72.39(5)	O(1W)-Eu(1)-O(2)	69.36(5)	O(1W)-Eu(1)-O(1)	93.80(5)
O(3)-Eu(1)-O(4)#2	137.39(4)	O(5)-Eu(1)-O(2W)	69.34(4)	O(2)-Eu(1)-O(1)	51.19(4)
O(5)-Eu(1)-O(1W)	74.90(5)	O(6)#1-Eu(1)-O(2W)	71.33(4)	O(2W)-Eu(1)-O(1)	137.24(4)
O(6)#1-Eu(1)-O(1W)	69.65(5)	O(1)#2-Eu(1)-O(2W)	77.41(4)	O(3)-Eu(1)-O(2W)	67.75(4)
		1-Gd			
Gd(1)-O(5)	2.3386(18)	Gd(1)-O(4)#2	2.411(2)	Gd(1)-O(1)	2.6107(18)
Gd(1)-O(6)#1	2.367(2)	Gd(1)-O(2)	2.477(2)	Gd(1)-O(3)	2.3909(19)
Gd(1)-O(1)#2	2.3792(19)	Gd(1)-O(1W)	2.478(2)	Gd(1)-O(2W)	2.548(2)
O(5)-Gd(1)-O(6)#1	87.19(7)	O(1)#2-Gd(1)-O(2)	121.98(6)	O(4)#2-Gd(1)-O(2W)	130.79(8)
O(5)-Gd(1)-O(1)#2	90.71(7)	O(3)-Gd(1)-O(2)	72.97(7)	O(2)-Gd(1)-O(2W)	129.27(7)
O(6)#1-Gd(1)-O(1)#2	146.73(7)	O(4)#2-Gd(1)-O(2)	99.76(8)	O(1W)-Gd(1)-O(2W)	127.04(7)
O(5)-Gd(1)-O(3)	136.75(7)	O(5)-Gd(1)-O(1W)	74.68(8)	O(5)-Gd(1)-O(1)	142.25(7)
O(6)#1-Gd(1)-O(3)	83.33(7)	O(6)#1-Gd(1)-O(1W)	69.07(8)	O(6)#1-Gd(1)-O(1)	124.27(6)
O(1)#2-Gd(1)-O(3)	75.65(7)	O(1)#2-Gd(1)-O(1W)	141.73(7)	O(1)#2-Gd(1)-O(1)	73.96(7)
O(5)-Gd(1)-O(4)#2	72.55(7)	O(3)-Gd(1)-O(1W)	137.89(7)	O(3)-Gd(1)-O(1)	73.40(6)
O(6)#1-Gd(1)-O(4)#2	136.73(8)	O(4)#2-Gd(1)-O(1W)	68.84(8)	O(4)#2-Gd(1)-O(1)	70.03(6)
O(1)#2-Gd(1)-O(4)#2	73.08(7)	O(2)-Gd(1)-O(1W)	69.33(7)	O(2)-Gd(1)-O(1)	50.89(6)
O(3)-Gd(1)-O(4)#2	136.94(7)	O(5)-Gd(1)-O(2W)	69.75(7)	O(1W)-Gd(1)-O(1)	96.09(7)
O(5)-Gd(1)-O(2)	143.40(7)	O(6)#1-Gd(1)-O(2W)	71.22(7)	O(2W)-Gd(1)-O(1)	135.51(6)
O(6)#1-Gd(1)-O(2)	74.19(7)	O(1)#2-Gd(1)-O(2W)	76.92(7)	O(3)-Gd(1)-O(2W)	67.23(7)
		1-Tb			
Tb(1)-O(5)	2.316(2)	Tb(1)-O(3)	2.387(2)	Tb(1)-O(1)	2.614(2)
Tb(1)-O(6)#1	2.337(2)	Tb(1)-O(2)	2.458(2)	Tb(1)-O(4)#2	2.373(2)
Tb(1)-O(1)#2	2.362(2)	Tb(1)-O(2W)	2.467(2)	Tb(1)-O(1W)	2.547(3)
O(5)-Tb(1)-O(6)#1	87.45(8)	O(1)#2-Tb(1)-O(2)	122.33(7)	O(3)-Tb(1)-O(1W)	131.27(9)
O(5)-Tb(1)-O(1)#2	89.73(8)	O(4)#2-Tb(1)-O(2)	73.32(8)	O(2)-Tb(1)-O(1W)	129.26(8)
O(6)#1-Tb(1)-O(1)#2	145.33(8)	O(3)-Tb(1)-O(2)	99.28(8)	O(2W)-Tb(1)-O(1W)	127.32(9)
O(5)-Tb(1)-O(4)#2	135.86(8)	O(5)-Tb(1)-O(2W)	75.45(9)	O(5)-Tb(1)-O(1)	142.44(7)
O(6)#1-Tb(1)-O(4)#2	82.77(8)	O(6)#1-Tb(1)-O(2W)	70.24(9)	O(6)#1-Tb(1)-O(1)	124.85(7)
O(1)#2-Tb(1)-O(4)#2	75.44(7)	O(1)#2-Tb(1)-O(2W)	141.73(8)	O(1)#2-Tb(1)-O(1)	74.09(8)
O(5)-Tb(1)-O(3)	73.06(8)	O(4)#2-Tb(1)-O(2W)	138.29(8)	O(4)#2-Tb(1)-O(1)	73.26(7)

O(6)#1-Tb(1)-O(3)	137.52(9)	O(3)-Tb(1)-O(2W)	68.48(9)	O(3)-Tb(1)-O(1)	69.91(7)
O(1)#2-Tb(1)-O(3)	73.51(8)	O(2)-Tb(1)-O(2W)	69.34(8)	O(2)-Tb(1)-O(1)	51.04(7)
O(4)#2-Tb(1)-O(3)	136.84(7)	O(5)-Tb(1)-O(1W)	69.35(8)	O(2W)-Tb(1)-O(1)	96.40(8)
O(5)-Tb(1)-O(2)	144.18(8)	O(6)#1-Tb(1)-O(1W)	70.27(9)	O(1W)-Tb(1)-O(1)	134.94(7)
O(6)#1-Tb(1)-O(2)	74.86(8)	O(1)#2-Tb(1)-O(1W)	76.42(8)	O(4)#2-Tb(1)-O(1W)	66.81(8)

Symmetry codes: **1-Eu**: #1 -x+1,-y,-z+2; #2 -x,-y,-z+2; **1-Gd**: #1 -x+1,-y+1,-z; #2 -x+2,-y+1,-z; **1-Tb**: #1 -x+1,-y,-z+2; #2 -x+2,-y,-z+2.

Table S2. The details of the contributions of orbital transitions for some electronic transitions with large oscillator strengths for ligand from the TD-DFT calculation.

	molecular orbital	Percentage (%)	Excitation energy (eV)	Excitation energy (nm)	Oscillator strength
Excited State 1:	41-> 43, H-1→ L 41-> 44, H-1→ L+1 42-> 43, H→ L 42-> 44, H→ L+1	39.52 5.66 46.56 8.01	4.568	271.5	0.0445
Excited State 2:	40-> 43, H-2→ L 40-> 45, H-2→ L+2	95.56 4.12	4.574	271.1	0.0001
Excited State 3:	41-> 43, H-1→ L 42-> 43, H→ L 42-> 44, H→ L+1	46.92 45.78 4.56	5.014	247.3	0.3598
Excited State 4:	38-> 43, H-4→ L 38-> 45, H-4→ L+2	96.45 2.23	5.852	211.9	0.0000
Excited State 5:	39-> 43, H-3→ L 41-> 43, H-1→ L 41-> 44, H-1→ L+1 42-> 44, H→ L+1	40.12 7.43 9.73 37.91	6.209	199.7	0.0993

Calculated output geometry obtained from static B3LYP/6-31G (d, p) geometry optimization and corresponding molecular orbital diagrams from TD-DFT electronic structure calculations for HL ligand.

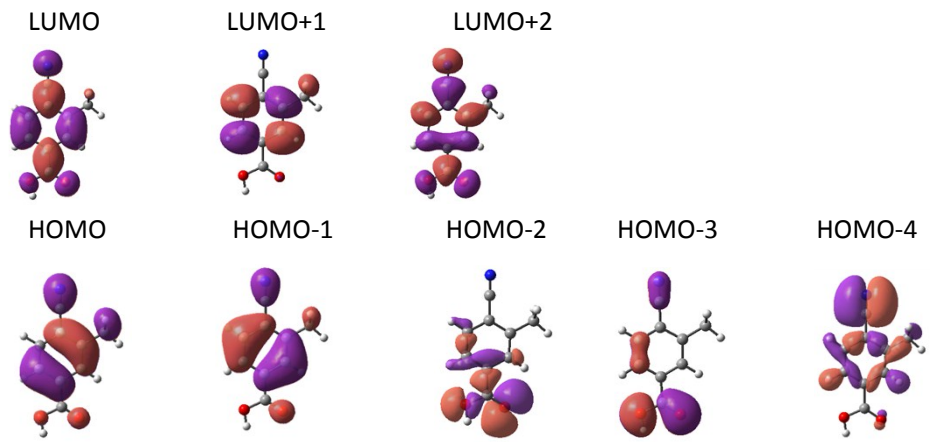

Table S3. Molar ratio of Eu^{3+} and Tb^{3+} ions in bimetallic-doped **1-Tbx/Eu1-x**.

	a	b	c	d	e
Eu^{3+}	0.0266	0.0395	0.0761	0.1024	0.1893
Tb^{3+}	0.9734	0.9605	0.9239	0.8976	0.8107